Proceeding of Ocean, Mechanical and Aerospace
-Science and Engineering-, Vol.2:1

November 23, 2015

Computational Study of Flow Structure after a Bluff Body with the Effect of Underneath Wavy Surface Using RNG-k-ε Model

Asral,[a,*] Jamaluddin Md Sheriff,[b] Kahar Osman, [b]

[a)] *Department of Mechanical Engineering, Universitas Riau, Pekanbaru, 28293, Indonesia*
[b)] *Faculty of Mechanical Engineering, Universiti Teknologi Malaysia, 81310 UTM Skudai Johor Bahru Malaysia*

*Corresponding author: asral@unri.ac.id

Paper History

Received: 10-October-2015
Received in revised form: 20-November-2015
Accepted: 23-November-2015

ABSTRACT

Present study, two-dimensional numerical solution for the same test condition has been performed by employing the turbulent model of RNG-k-ε to simulate the flow pattern after a rectangular bluff body of which has height to width ratio of two in various wavy surface conditions and Reynolds numbers. Sinusoidal surfaces were chosen for wavy condition to represent the wavy boundary. Range of Reynolds numbers were 1480 to 3300 and the waves amplitude were 0.13 of the bluff body height (0.13D), 0.33D and 0.67D. Comparisons were made against flow over the flat surface for the same flow condition**.** For most cases studied, two vortices always present in the region in the vicinity close to the bluff body. Larger size of vortices appears in the middle area than those in the upper area of the flow and less vortices occurs in the lower area**.** For low amplitude wave, the flow tends to follow the wave and resulted in large streamwise and spanwise negative velocity zone behind the bluff body. As the wave amplitude increases, the size of this negative velocity region will reduce**.** Otherwise. all wavy surface condition with the variation of amplitude also increases the strength of vortices as the Reynolds number increases occurred in the middle area to provide with the velocity profile along centerline. In general, the numerical solutions were in good result to calculate the velocity pattern.

KEY WORDS: *Vortex, reattachment length, wave, wake, bluff body*

1.0 INTRODUCTION

The profile of flow around bluff bodies such as cubes, rectangular and circular cylinders, and flat plates are relevant to many engineering designs, such as constructions under the action of wind loading like building, chimneys and water tank tower, steel tower suspension bridges or marine structures under the action of water loading. Wind driving forces on infrastructures, located nearby coastal region are considered to be an important parameter in design. The study of flow structures, i.e formation of vortex and free shear layer due to wind loading have been conducted by many researchers. However, there is lack of references for data of flow structure on the effect of water wave to the flow structures. This study will contribute numerical data of flow structure with the effect of water wave. The objective of this current study is to investigate the effect of wavy boundaries upon profile of flow after a bluff body for various amplitude conditions.

Experimental study on the characteristics of flow in the wake region of bluff body with the ground effect has been investigated by Kim and Gerops (1998). The author studied the effect of various ground clearances on the flow around a variety of bluff bodies. Barlow *et al.* (2001) presented the ground effect with different aspect ratios, varying ground clearances, and different levels of underbody roughness were performed in wind tunnel experiment. Jefrey *et al.* (1984) identified the separated region, an attached boundary layer, and a free shear layer formed by the detachment of the boundary layer from the wave surface. Zhang *et al.* (2005) reported the sinusoidal surface geometry significantly modifies the near –wake structure and strongly controls the three-dimensional vortices formed in the near wake. Larose and Auteuil (2006) demonstrated that the aerodynamics of bluff bodies with sharp edges can be sensitive to Reynolds number effects. Schewe (2001) reported that Reynolds-number effects can be have drastic consequences on the unsteady behaviour and on the fluid forces acting on an aeroelastic system. Tieleman *et al.* (2003) measured the pressure and area load fluctuations on the top surface of a surface-mounted prism in

seven different wind tunnel configurations. Two groups of eight pressure taps placed in critical areas are considered. The characterization is presented in terms of the mean, root mean square, and peak values, probability distributions, peak durations, and correlation coefficients. They conclude that the quality of wind tunnel experiment is depends greatly on the incident turbulence for assessment of wind loads on low-rise structures.

Cause to the cost and time to do the full scale and practical investigation then the computational wind engineering has been developed to evaluate the interaction between wind and structure numerically. Computational fluid modeling in wake region has been widely used by many researchers in their investigation. Bouris and Bergeles (1999). Selvarajan, Tulapurkara, and Ram (1998) reported the amplitude of shear stress along the wall increases and pressure decreases with increase in Reynolds number. Such investigation include the study *k-ε* model, Lakehal (1998), Shimada and Ishihara (2002), Zhou and Stathopolus (1997), Delaunay et al (1995), Johansen *et al.* (2004), Lakehal and Rodi (1997) and with Large eddy simulation (LES) method by Murakami and Mochida (1995). As the LES can be applied to 3D flow simulation and needs finer grid arrangement, it takes more computational time than the *k-ε* method which can only be applied to 2D where these feature applicable to simulate the flow profile over simetrycal bluff body for FLUENT application. Therefore, the k-ε model method is very attractive to wind engineers since it needs much less computational power than the LES method. In the *k-ε* model, it is three method available in FLUENT that is Standard, RNG, and Reliazible method. For standard model many researcher have been performed the investigation with improved the grid and the calculation to increased the predictive capability considerably. However, as RNG and Reliazible method are available in FLUENT that the features of them can improve the desirable result easily.

2.0 NUMERICAL APPROACH

In principle, the basic equation used in this case study is continuity equations and the momentum equations written as follows:

$$\frac{\partial \rho}{\partial t} + \nabla . (\rho \vec{v}) = S_m \quad (1)$$

$$\frac{\partial}{\partial t}(\rho u_i) + \frac{\partial}{\partial x_j}(\rho u_i u_j) = -\frac{\partial \rho}{\partial x_i} + \frac{\partial}{\partial x_j}\left[\mu\left(\frac{\partial u_i}{\partial x_j} + \frac{\partial u_j}{\partial x_i} - \frac{2}{3}\delta_{ij}\frac{\partial u_l}{\partial x_l}\right)\right] + \frac{\partial}{\partial x_j}(-\overline{\rho u_i' u_j'}) \quad (2)$$

The turbulent kinetic energy, *k* transport equation for The RNG $k-\varepsilon$ model, given by:

$$\frac{\partial}{\partial t}(\rho k) + \frac{\partial}{\partial x_i}(\rho k u_i) = \frac{\partial}{\partial x_j}\left(\alpha_k \mu_{eff}\frac{\partial k}{\partial x_j}\right) + G_k + G_b - \rho\varepsilon - Y_M + S_k \quad (3)$$

and for dissipation rate, ε written by:

$$\frac{\partial}{\partial t}(\rho\varepsilon) + \frac{\partial}{\partial x_i}(\rho\varepsilon u_i) = \frac{\partial}{\partial x_j}\left(\alpha_\varepsilon \mu_{eff}\frac{\partial \varepsilon}{\partial x_j}\right) + C_{1\varepsilon}\frac{\varepsilon}{k}(G_k + C_{3\varepsilon}G_b) - C_{2\varepsilon}\rho\frac{\varepsilon^2}{k} - R_\varepsilon + S_\varepsilon \quad (4)$$

In these equations, G_k represents the generation of turbulence kinetic energy due to the mean velocity gradients. G_b is the generation of turbulence kinetic energy due to buoyancy.Y_M represents the contribution of the fluctuating dilatation in compressible turbulence to the overall dissipation rate. The quantities α_k and α_ε are the inverse effective Prandtl numbers for k and ε , respectively. S_k and S_ε are user-defined source terms. The model constants $C_{1\varepsilon}$ and $C_{2\varepsilon}$ have values derived analytically by the RNG theory. These values, used by default in FLUENT, are: $C_{1\varepsilon}$ =1.42, $C_{2\varepsilon}$ = 1.68 C_μ = 0.0845

For all test cases Fluent was employed to predict the flow pattern and condition. Two-dimensional model was used to simulate the flow against the bluff body on the wavy surfaces. The flow was simulated in a numerical tunnel. The geometry and typical boundary conditions are shown in Figure 1. No slip boundary conditions were imposed on all walls. As seen, a rectangular bluff body with a side D located at (31.5D,3.17D) is expose to a constant free stream velocity U. The flow is described in cartesian coordinate system (x,y) in which the x –axis is aligned with the inlet flow direction and y axis is perpendicular to the flow direction. The origin of the coordinate system is located at the left bottom of the tunnel, see Figure 1.The ratio of the length of the test section to the height of the bluff body is 63. The ratio of the height of the test section to the height of the bluff body is 14.5. The uniform flow conditions at inlet for Reynolds number 1480, 1850, 2775, and 3300 were used in this study. Air is flowing through the wavy surface from the right and solutions were forced in order to study the characteristic of the vortex in the wake region.

In order to simulate the effect of wavy surface to the flow against the bluff body, sinusoidal surfaces with different amplitude were used. The RNG-*k-ε* model was used to capture the turbulent phenomenon. The wavy surface condition is employed in the three variations of amplitude and also flat surface as comparison. Simulations were left to run until steady state conditions were reached for normal wind conditions.

3.0 VERIFICATION MODEL

In order to choose the most suitable turbulence model, arbitrary test case was done using several turbulence models. Comparisons were made with Johansen, Wu, and Shyy (2004). From Figure 2, RNG-*k-ε* model was chosen since it correlated well with the publish data. Further test was done by computing RNG-*k-ε* results with those obtained from PIV technique, based on actual model. From Figure 3 to 5, RNG-*k-ε* model also correlated well with the experimental results.

4.0 RESULTS AND DISCUSSION

The fluid flow passing the bluff body is divided into upward and downward flows at upwind face of the bluff body. To characterize the flow behavior reattachment length will be define as the distance from the downwind face of the bluff body to the point where the separated flow returned to its original datum. In this discussion, the datum is chosen to be at the bottom face or top

face of the bluff body.

In present study, the discussions are revealed for location of bluff body above the down wave of wavy surface, as shows in Figure 6 to Figure 13. Tabulated data of location of vortex and reattachment length of the flow for various Reynolds numbers are presented as in Table 1. For all condition the effects of Reynolds number shows difference in respond and sensitivity as seen along centerline. All result exhibited the sensitivity reduces as the amplitude of the wave increase due to difference in slope of wave. Wave with the slightly slope to be more sensitive due to the flow follow the wave, it could accelerate the fluid flow. However, wavy surface with the high amplitude could decelerate the flow in the under area of bluff body then the flow changed the direction, this phenomena specially occurred for downward flow.

For the highest amplitude of the wave shows the insignificant alterations to the velocity profile. However, flow structure after bluff body shows many alterations. As the Reynolds numbers increases the position and size of vortices are change also the reattachment flow tend only occurred for separated flow of downward flow. In the other hand, the variation of amplitude of wavy surface was employed in double, that is more possible to occur of this phenomenon. For all case study, variations in Reynolds number can change the structure of flow after rectangular bluff body, similar results are proposed by schewe and Larsen (1998).

5.0 CONCLUSION

In this case study, two vortices always present in the region in the vicinity close to the bluff body. Larger size of vortices appears in the middle area than those in the upper area of the flow and less vortices occurs in the lower area. For low amplitude wave, the flow tends to follow the wave and resulted in large streamwise and spanwise negative velocity zone. As the wave amplitude increases, the size of negative velocity region will reduce. In general, the numerical solutions were in good result to calculate the velocity pattern.

6. 0 REFERENCES

1. Barlow, Jewel B., Guterres, Rui and Ranzenbach, Robert., (2001). Experimental parametric study of rectangular bodies with radiused edges in ground effect, *Journal of Wind engineering and Indsutrial Aerodynamics*, 89:1291-1309.
2. Bouris, D., and Bergeles, G., (1999). 2D LES of vortex shedding from a square cylinder, *Journal of Wind Engineering and Industrial Aerodynamics*, 80: 31-46.
3. Bearmen, P.W., (1997). Near Wake Flows Behind Two-and Three-Dimensional Bluff Bodies, *Journal of Wind Engineering and Industrial Aerodynamics*, 69-71: 33-54.
4. Buckles, Jeffrey, Hanratty, Thomas J., and Adrian, Ronald J., (1984). Turbulent Flow Over Large-Amplitude Wavy Surfaces, *Journal Fluid Mechanics*, 140: 27-44.
5. Delaunay, D., Lakehal, D., and Pierrat, D. (1995).. Numerical Approach for Wind Loads Prediction on Buildings and Structures, *Journal of Wind Engineering and Industrial Aerodynamics*. 57: 307-321
6. Johansen, Stein T., Wu, Jiongyang, and Shyy, Wei., (2004). Filter-based unsteady RANS computations, *International Journal of Heat and Fluid Flow*, 25:10-21.
7. Kim, M.S, and Geropp. D. (1998). Experimental investigation of the ground effect on the flow around some two-dimensional bluff bodies with moving-belt technique, *Journal of Wind Engineering and Industrial Aerodynamics*, 74-76: 511-519.
8. Lakehal, D. (1998). Application of the *k-ε* Model to Flow Over a Building Placed in Different Roughness Sublayers, *Journal of Wind Engineering and Industrial Aerodynamics* .73: 59-77.
9. Larose, G.L., and D'Auteuil, A. (2006). On the Reynolds Number Sensitivity of the Aerodynamics of Bluff Bodies with Sharp Edges, *Journal of Wind Engineering and Industrial Aerodynamics*. 94:365–376.
10. Murakami, Shuzo, Mochida, Akashi, and Sakamoto, Shigehiro (1997). CFD Analysis of Wind-Structure Interaction for Oscillating Square Cylinders, *Journal of Wind Engineering and Industrial Aerodynamics*.72 :33-46
11. Rodi, W., (1997). Comparison of LES and RANS calculations of the flow around bluff bodies, *Journal of Wind Engineering and Industrial Aerodynamics*, 69-71: 55 75.
11. Schewe, Gunter (2001). Reynolds-number Effects in Flow Around More-or-Less Bluff Bodies, *Journal of Wind Engineering and Industrial Aerodynamics*. 89: 1267–1289.
12. Selvarajan, S., Tulapurkara, E.G., and Ram, V.Vasanta (1998). A Numerical Study of Flow Through Wavy-Walled Channels, *Int. J. Numer. Meth. Fluids*. 26: 519-531.
13. Simada, K., and Ishihara, T. (2002). Application of a Modified *k-ε* Model to the Prediction of Aerodynamic Characteristic of Rectangular Cross-Section Cylinders, *Journal of Fluids and Structures*. 16(4): 465-485.
14. Schewe, Gunter, and Larsen, Allan (1998). Reynolds Number Effects in the Flow Around a Bluff bridge Deck Cross Section, *Journal of Wind Engineering and Industrial Aerodynamics*. 74-76: 829-838.
15. Tieleman, Henry W., Ge, Zhongfu, Hajj, Muhammad R., and Reinhold, Timothy A. (2003). Pressures on a Surface-Mounted Rectangular Prism Under Varying Incident Turbulence, *Journal of Wind Engineering and Industrial Aerodynamics*. 91 :1095–1115.
16. Zhou, Yongsheng, and Stathopoulos, Ted (1997). A New Technique for the Numerical Simulation of Wind Flow Around Buildings, *Journal of Wind Engineering and Industrial Aerodynamics*. 72:137 147.
17. Zhang, Wei, Daichin, and Lee, Sang Joon. (2005). PIV Measurement of The Near-Wake Behind a Sinusoidal Cylinder, *Springer-Verlag*.10.1007/s00348-005-0981-9.

Table 1: Location of recirculation zone and reattachment length for various Reynolds numbers.

Positions	Surfaces	Experimental				
		Location of Recirc. Zone, X/D			Reattach. Length, X/D	
		Upper Area	Middle Area	Lower Area	Upward Flow	Downward Flow
Re = 1480	Flat	0.3-0.6			0.6	1.6
	Wave-1	2-2.4	0.3-0.8	-	-	0.6
	Wave-2	-	-	-	-	3.3
	Wave-3	0-0.3	0.9-1.3	-	-	1.2
Re = 1850	Flat	-	-	0.1-0.5	-	0.4
	Wave-1	-	0.8-1.4	0-0.3	-	0.4
	Wave-2	-	-	-	-	4.1
	Wave-3	-	0.7-1.1	-	-	1
Re = 2775	Flat	0.4-0.8	-	-	0.7	-
	Wave-1	0.1-0.4	1.3-1.6	-	0.4	1.2
	Wave-2	-	-	-	-	4.1
	Wave-3	-	-	-	-	1.3
Re = 3300	Flat	0.3 - 1.2	0.3 - 0.9	1.7 - 2.5	2.3	0.5
	Wave-1		0.6-1.1		-	-
	Wave-2	0.1-0.4	1-1.3	-	0.4	1.2
	Wave-3	-	-	-	-	1.2

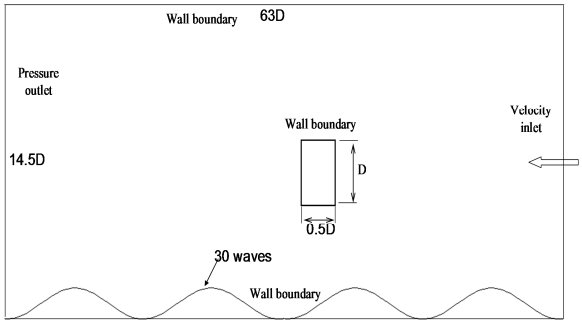

Figure 1: Geometry and typical boundary conditions.

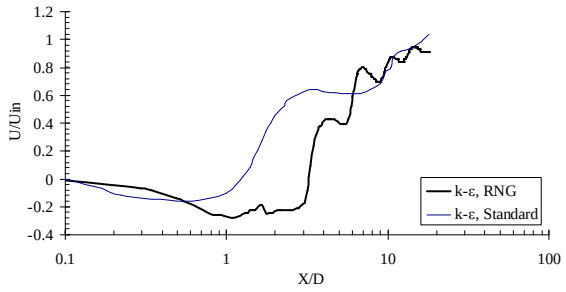

Figure 2: Streamwise velocity components along centerline. *k-ε* RNG from current study and *k-ε*, standard from Johansen *et.al*, (2004).

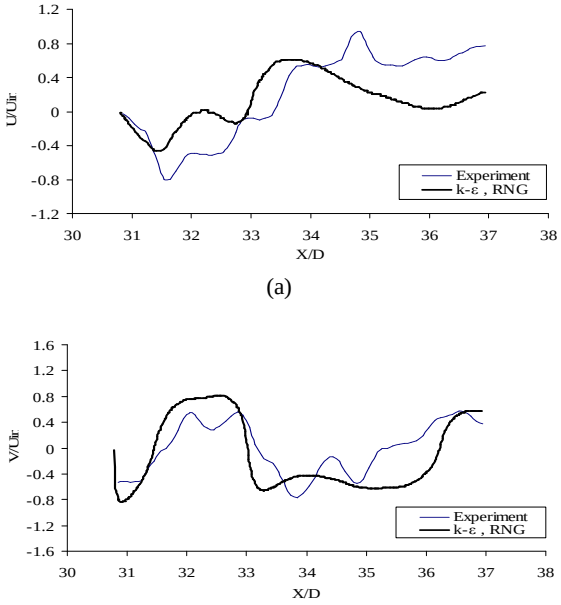

Figure 3: Comparison of velocity components along centerline for experimental and *k-ε*, RNG model for wave-1, (a) streamwise, (b) spanwise.

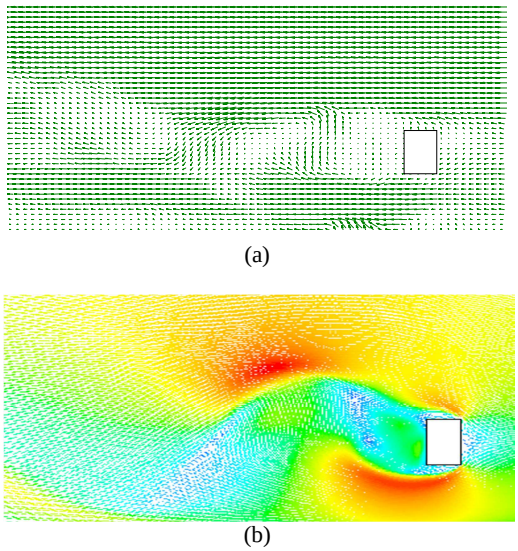

Figure 4: Comparison of velocity vector for: flat surface, (a) experiment, (b) *k-ε*, RNG model

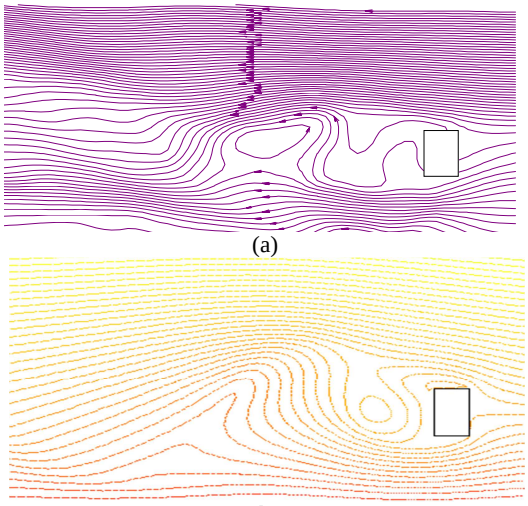

(a)

(b)

Figure 5: Comparison of streamline for: flat surface, (a) experiment, (b) *k-ε*, RNG - model.

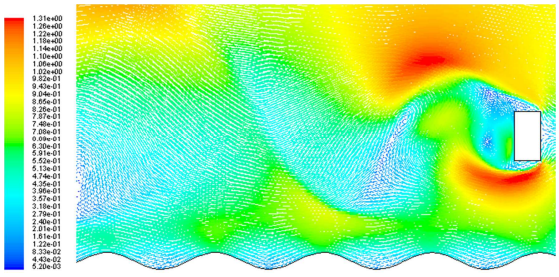

(a) Wave-1

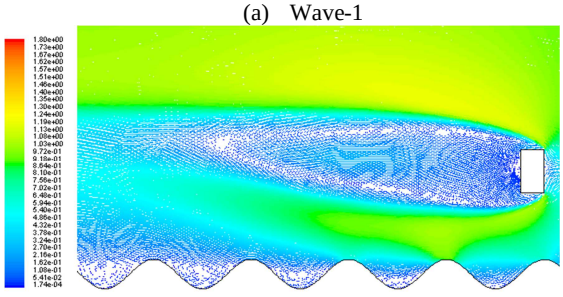

(b) Wave-2

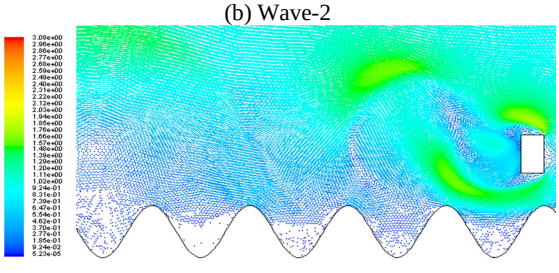

(c) Wave-3

Figure 6: Velocity vector for various amplitude of wavy surface for Reynolds Number, Re = 1480, (a) – (c).

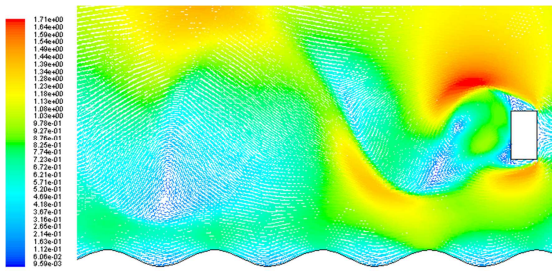

(b) Wave-1

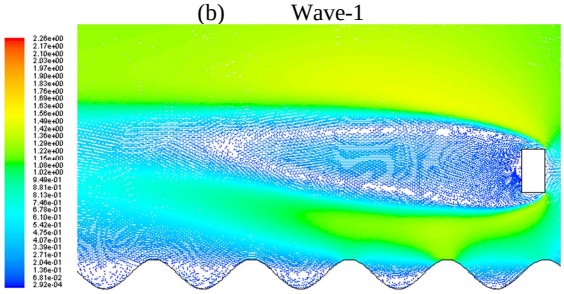

(b) Wave-2

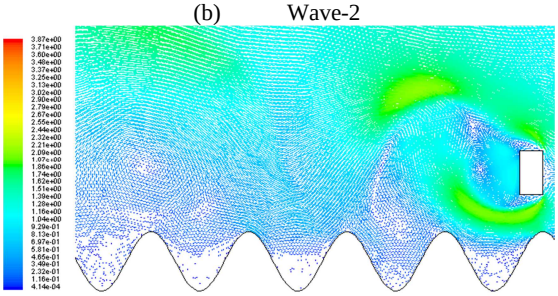

(c) Wave-3

Figure 7: Velocity vector for various amplitude of wavy surface for Reynolds Number, Re = 1850, (a) – (c).

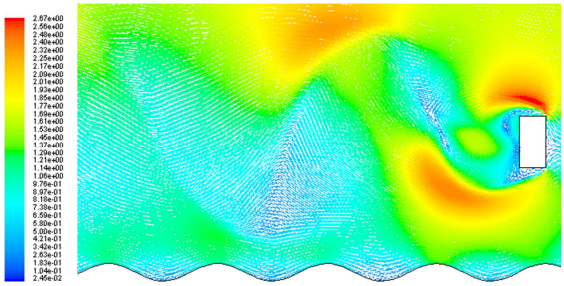

(a) Wave-1

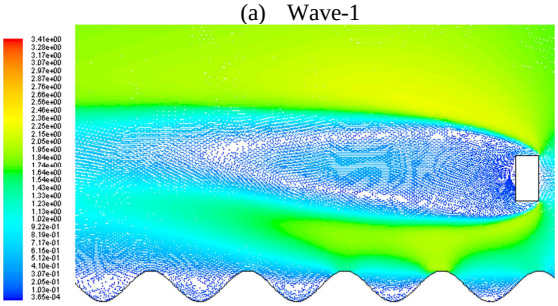

(b) Wave-2

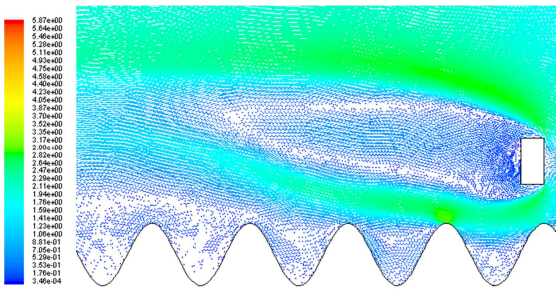

(c) Wave-3

Figure 8: Velocity vector for various amplitude of wavy surface for Reynolds Number, Re = 2775, (a) – (c).

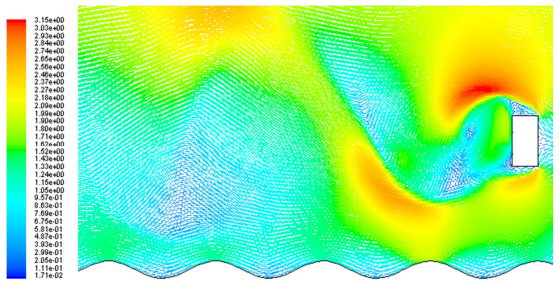

(a) Wave-1

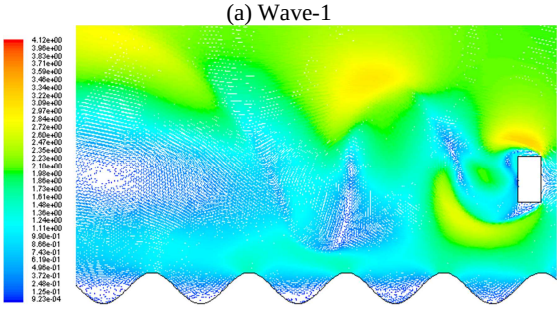

(b) Wave-2

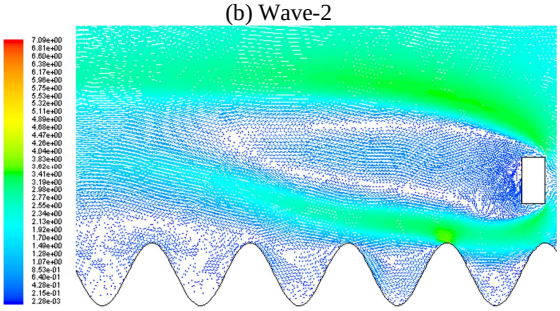

(c)Wave-3

Figure 9: Velocity vector for various amplitude of wavy surface for Reynolds Number, Re = 3300, (a) – (c).

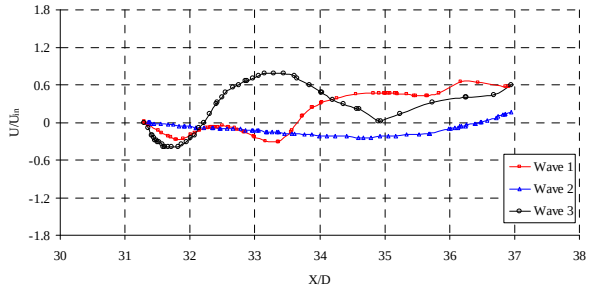

(a)

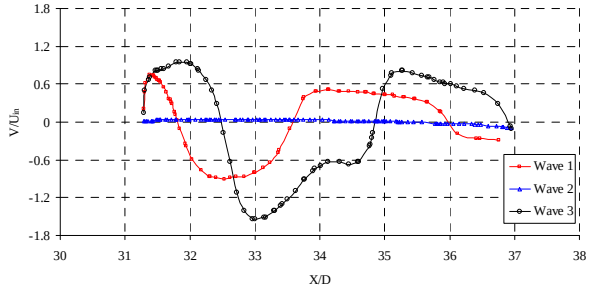

(b)

Figure 10: Streamwise (a) and spanwise (b) velocity components at centerline for various amplitudes of wavy surface, Re = 1480

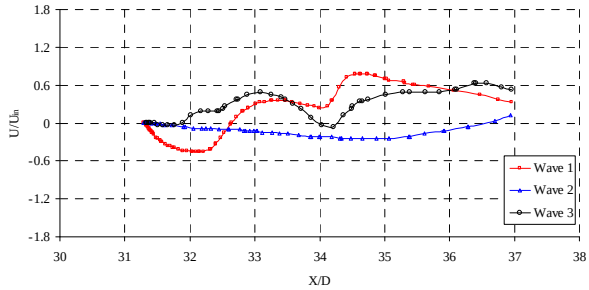

(a)

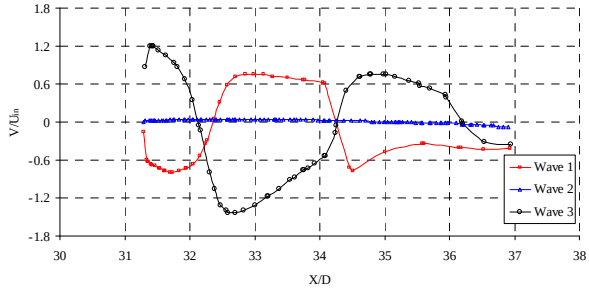

(b)

Figure 11: Streamwise (a) and Spanwise (b) velocity components at centerline for various amplitudes of wavy surface, Re = 1850

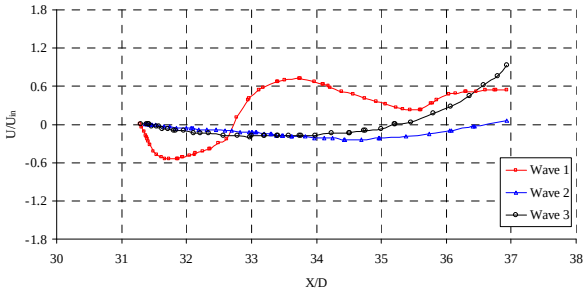

(a)

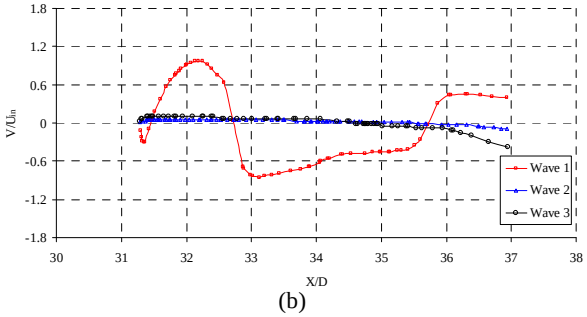

(b)

Figure 12: Streamwise (a) and spanwise (b) velocity components at centerline for various amplitudes of wavy surface, Re = 2775.

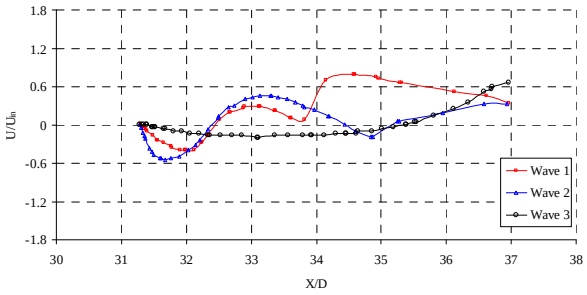

(a)

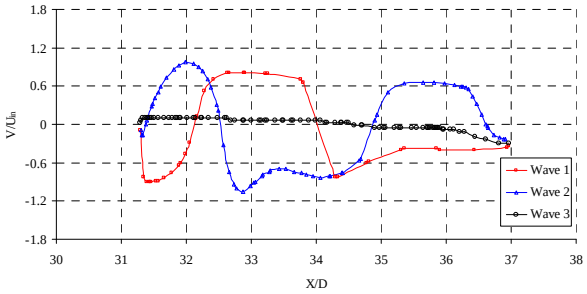

(b)

Figure 13: Streamwise (a) and spanwise (b) velocity components at centerline for various amplitudes of wavy surface, Re = 3300.